Biosensors and Bioelectronics 55 (2014) 99–105

Contents lists available at ScienceDirect

Biosensors and Bioelectronics

journal homepage: www.elsevier.com/locate/bios

Approaches to label-free flexible DNA biosensors using low-temperature solution-processed InZnO thin-film transistors

Joohye Jung [a], Si Joon Kim [a], Keun Woo Lee [a,b], Doo Hyun Yoon [a], Yeong-gyu Kim [a], Hee Young Kwak [a], Sreekantha Reddy Dugasani [b], Sung Ha Park [b,*], Hyun Jae Kim [a,**]

[a] School of Electrical and Electronic Engineering, Yonsei University, 50 Yonsei-ro, Seodaemun-gu, Seoul 120-749, Republic of Korea
[b] Department of Physics and SKKU Advanced Institute of Nanotechnology (SAINT), Sungkyunkwan University, Suwon, Gyeonggi-do 440-746, Republic of Korea

ARTICLE INFO

Article history:
Received 23 September 2013
Received in revised form
19 November 2013
Accepted 28 November 2013
Available online 10 December 2013

Keywords:
Flexible biosensors
Oxide TFTs
DNA
Solution-process
In–Zn–O

ABSTRACT

Low-temperature solution-processed In–Zn–O (IZO) thin-film transistors (TFTs) exhibiting a favorable microenvironment for electron transfer by adsorbed artificial deoxyribonucleic acid (DNA) have extraordinary potential for emerging flexible biosensor applications. Superb sensing ability to differentiate even 0.5 μL of 50 nM DNA target solution was achieved through using IZO TFTs fabricated at 280 °C. Our IZO TFT had a turn-on voltage (V_{on}) of −0.8 V, on/off ratio of 6.94×10^5, and on-current (I_{on}) value of 2.32×10^{-6} A in pristine condition. A dry-wet method was applied to immobilize two dimensional double crossover tile based DNA nanostructures on the IZO surface, after which we observed a negative shift of the transfer curve accompanied by a significant increase in the I_{on} and degradation of the V_{on} and on/off ratio. As the concentration of DNA target solution increased, variances in these parameters became increasingly apparent. The sensing mechanism based on the current evolution was attributed to the oxidation of DNA, in which the guanine nucleobase plays a key role. The sensing behavior obtained from flexible biosensors on a polymeric substrate fabricated under the identical conditions was exactly analogous. These results compare favorably with the conventional field-effect transistor based DNA sensors by demonstrating remarkable sensitivity and feasibility of flexible devices that arose from a different sensing mechanism and a low-temperature process, respectively.

1. Introduction

Biosensors are analytical devices used to detect biological elements harnessing the exquisite sensitivity and binding specificity of biology such as proteins, enzymes, antibodies, and nucleotides. Potential uses incorporate a substantial percentage of every conceivable analytical task encompassing environmental monitoring, medical diagnostics, pathogen detection, food safety, and anti-bioterrorism strategies (Boon et al., 2002; DeRisi et al., 1997; Honeychurch et al., 2007; Jung et al., 2013; Kim et al., 2012; Newman and Turner, 2005; Sharma and Mutharasan, 2013; Singh et al., 1988; Turner, 2013; Xuan et al., 2012; Yan and Tang, 2010; Zhang et al., 2007; Zuo et al., 2010). The detection of nucleic acid targets has received considerable attention among several types of biosensors due to its importance in the investigation of the gene (Zhang et al., 2007). Although a number of deoxyribonucleic acid (DNA) bio sensing approaches have been studied, there is still a constant desire for more inexpensive, simple, sensitive, stable, and portable DNA biosensors. Most of the conventional DNA biosensors imposed fluorescence detection of labeled targets or probes causing attendant limitations of expensive and large laser scanners, limited field deployability, and restricted sensitivity (DeRisi et al., 1997; Sharma and Mutharasan, 2013; Singh et al., 1988; Zuo et al., 2010).

Reflecting on the former biosensor development, one can clearly see the impact of label-free methods (Honeychurch et al., 2007; Jung et al., 2013; Kim et al., 2012; Xuan et al., 2012; Yan and Tang, 2010). In particular, field-effect transistor (FET) based DNA biosensors have been studied extensively owing to their various advantages over other methods, including direct transduction and high sensitivity. Furthermore, small-sized and high-density FET arrays have an intuitive appeal as portable or pocket-sized biosensors, and this has driven the diverse range of applications reported in the literature (Jung et al., 2013; Kim et al., 2012; Yan and Tang, 2010). One of the most promising candidates is solution based metal oxide thin-film transistors (TFTs) due to their various merits such as low production costs, high reliability, easy reproducibility, in-situ analysis, and broad adaptability to fabrication methods, which even includes the stiffness of substrates (Jung et al., 2013; Kim et al., 2012, 2013b; Reyes et al., 2011).

* Corresponding author.
** Corresponding author.
E-mail addresses: sunghapark@skku.edu (S.H. Park), hjk3@yonsei.ac.kr (H.J. Kim).

0956-5663/$ - see front matter © 2013 Elsevier B.V. All rights reserved.
http://dx.doi.org/10.1016/j.bios.2013.11.076

In previous work, we have represented solution-processed In–Ga–Zn–O (IGZO) TFTs as alternative DNA biosensors with acceptable sensing capability for the first time (Kim et al., 2012) and complemented their sensitivity and environmental stability through structural engineering (Jung et al., 2013). Although these results manifested the feasibility of metal oxide-based TFTs as DNA biosensors, IGZO TFTs still have some inherent issues, for instance, an excessively high processing temperature of the IGZO layer and a sensing mechanism based on a sole trigger, the electrostatic force between the targets and the detection area.

The high processing temperature required to transform liquid phase material into solid phase IGZO thin film causes hardship to them being applied in flexible biosensors. In addition, sensing behavior depends on electrostatic force, excluding any chemical interactions, has ambiguous electrical responses for solvents, detected DNA targets, and external noises. As a result, quantitative analysis of samples that allows direct comparison between each sample prepared at different times or under different conditions is hardly used (Jung et al., 2013; Kim et al., 2012).

Among other metal oxide semiconductors, In–Zn–O (IZO) has been known as a favorable material for immobilization of biomolecules with low isoelectric points such as DNA or enzymes through electrostatic interaction without any electron mediator because of its high isoelectric point around 8.7–8.9. Its biocompatibility, nontoxicity, and smooth surface also deserve consideration (Hammarberg et al., 2009; Kosmulski, 2001).

In this work, we introduce low-temperature solution-processed IZO TFTs with a construction temperature of only 280 °C, which is a decisive factor in flexible devices being able to compensate for the aforementioned limitations. We investigated not only the immobilization and detection of artificial DNA nanostructures on the IZO channel, but also performed a quantitative analysis of DNA targets, paying special attention to its sensing mechanism attributed to DNA oxidation. On the basis of the results, we demonstrated the feasibility of solution-processed IZO TFTs as flexible DNA biosensors with high reliability and practicality.

2. Experimental procedure

2.1. Preparation of the IZO solution

Indium nitrate hydrate [$In(NO_3)_3 \cdot xH_2O$] and zinc acetate dihydrate [$Zn(CH_3COO)_2 \cdot 2H_2O$] were used as precursors to prepare the IZO solution. The precursors were dissolved in a 2-methoxyethanol (2ME) solvent. Then nitric acid [HNO_3] was added in a dropwise manner to achieve a homogeneous solution. The mixture was stirred for 1 h at 60 °C, and aged another 24 h. After all these procedures, the IZO solution was prepared with a molarity of 0.3 M.

2.2. Fabrication of biosensors

We fabricated a bottom-gate, top-contact type of TFT structure on a heavily doped p-type Si wafer with a 1200-Å-thick thermally grown SiO_2 to evaluate the sensing ability. The substrate was cleaned via a standard cleaning method and then spin-coated with the IZO solution at 3000 rpm for 30 s, followed by 5 min of pre-annealing at 100 °C and 4 h of annealing at 280 °C in ambient air. Deposition of Mo electrode was executed by sputtering with a length (L) of 150 μm and a width (W) of 1000 μm. In the case of a flexible biosensor, exactly the same fabrication process was applied on a polyimide substrate on which SiO_x gate insulator, Mo gate electrode, and SiO_x–SiN_x buffer layer were deposited as depicted in Supplementary Fig. S1.

2.3. Solvent effect of biosensors

Three types of solvents, chlorobenzene, ethanol, and deionized (DI) water which represent nonpolar solvent, polar solvent, and water-based solvent respectively were considered for the DNA solution. Using a micropipette, a single drop of each solvent was placed on the exposed IZO channel surface. Prior to all the electrical measurements, the devices were kept in ambient air for a few minutes to evaporate the solvents.

2.4. Preparation of DNA sample solution

Double crossover (DX) DNA nanostructure was artificially designed for the test by free-solution annealing as follows. Synthetic oligonucleotides were purchased from Bioneer Co. Ltd. (Korea), and purified by high performance liquid chromatography (HPLC). For annealing, stoichiometric quantities of each strand were pipetted into a test tube along with a physiological buffer, $1 \times$ TAE/Mg^{2+}, a mixture of tris-acetate-ethylendiaminetetraacetic acid (TAE), 40 mM tris-base, 1 mM EDTA (pH 8.0), and 12.5 mM $Mg(acetate)_2$. The samples were then cooled slowly from 95 °C to 25 °C by placing the test tube in 2 L of boiled water in a styrofoam box for 24 h to facilitate hybridization (Jung et al., 2013; Shin et al., 2011). Detailed base sequences of DX tiles and atomic force microscopy (AFM) images of DX DNA nanostructures are shown in Supplementary Fig. S2. The DNA nanostructures were then restored and delivered in a non-aqueous solvent, ethanol, using the dry-wet method (DWM) for minimizing the possible detriment to the TFTs during DNA immobilization (Jung et al., 2013; Kim et al., 2012; Lee et al., 2011). The specific procedure of the DWM was described in our previous study (Kim et al., 2012).

2.5. Characterization of biosensors

The prepared DX DNA sample solution was dropped onto the exposed IZO channel with a micropipette, and the device was then set in ambient air enabling evaporation of the solvent and the physical immobilization of the DX DNA nanostructures. The electrical characteristics of the devices were measured in the dark under ambient conditions using a semiconductor parameter analyzer (HP 4156C; Hewlett Packard, Palo Alto, CA).

3. Results and discussion

In the present study, we used two dimensional (2D) DX tile based DNA nanostructures which consisted of two repeating DX tiles as shown in Supplementary Fig. S2(a). This allows accurate control of analyte for sensor to figure out the origin of sensing mechanism. A unit DX tile (DX1 and DX2) was organized in two DX junctions and two parallel duplexes were tied up. Supplementary Fig. S2(b) represents the schematic diagram of the DX nanostructures. Supplementary Fig. S2(c) and (d) shows the AFM images of pristine IZO and DNA immobilized IZO, respectively, and also the insets of the bottom left, the noise-filtered 2D spectrum images (scan size 150×150 nm^2) according to fast Fourier transform, show no sign of periodicity for pristine IZO and clear periodicity indication for DX DNA. The theoretical dimensions of each DX tile were 12.6 nm in length and 4.0 nm in width. From AFM section measurements, the experimental values of length and width were 12.1 nm and 4.1 nm which are in good agreement with the theoretical values.

At first, we considered the electronic responses of the solution-processed IZO TFTs for exposure to various solvents. Transistor characteristics such as transfer curve as a function of applied gate voltage are known to be sensitive to changes in the environment

around the channel including molecular presence. All of the devices were measured with a gate voltage swept from −30 to 30 V and a fixed drain voltage of 10.1 V. Fig. 1 shows the temporal variation of the transfer curves that confirm each step of the recovery process after exposure to a solvent. Note that the device treated with chlorobenzene and the one treated with ethanol both exhibited a sufficient recovery of the off current (I_{off}) and almost no change in the on current (I_{on}) compared to those exposed with DI water after 5 min. It has been determined that solvent molecules adsorbed on the metal oxide surface accumulate extra electrons due to its polarity or electronegativity in our earlier study (Kim et al., 2013a). Furthermore, even the solvent has a high dielectric constant, the donor effect occurred by a highly volatile substance such as, ethanol disappears rapidly. In this respect, chlorobenzene and ethanol are appropriate for DWM in our study.

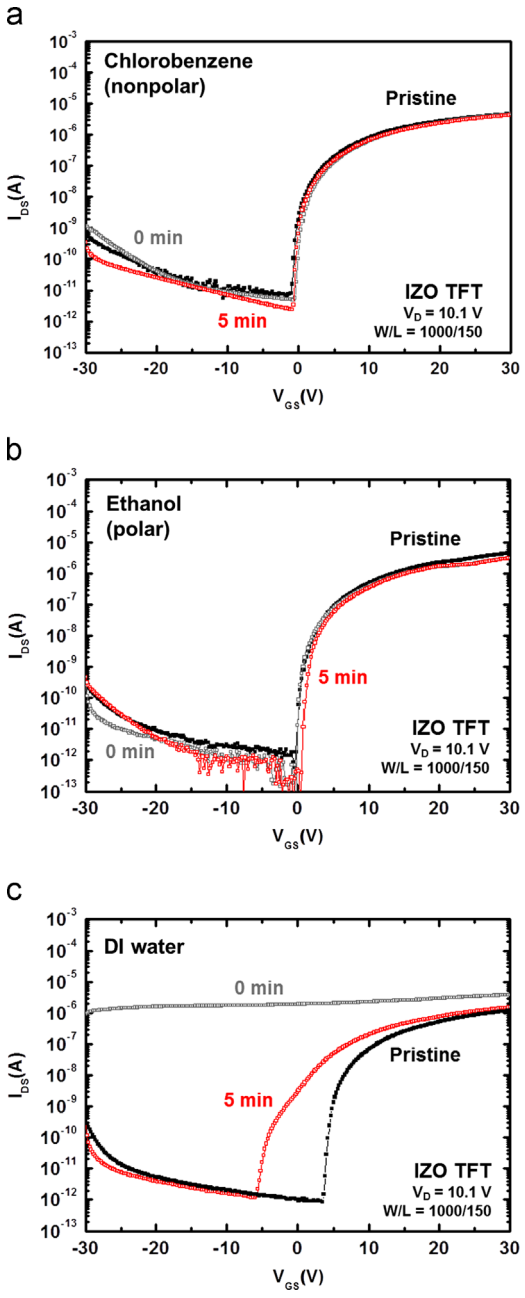

Fig. 1. Temporal variation of transfer characteristics of the IZO TFT exposed to (a) chlorobenzene, (b) ethanol, and (c) DI water.

The transfer characteristics of IZO TFTs upon DNA immobilization with varying DNA concentrations of 50, 100, 200, and 400 nM are shown in Fig. 2. In general, a DNA immobilized TFT tends to be more conductive attending a very significant negative shift of the turn-on voltage (V_{on}), and a decrease of the on/off ratio without recovery. Specifically in the 50 nM immobilized sensor, V_{on} and the on/off ratio shifted from −0.8 V to −8.2 V and from 6.94×10^5 to 6.04×10^4, respectively. This behavior became more severe as the concentration of DNA increased, with I_{on} as high as 122.13 μA being realized when DNA concentration was 400 nM. Furthermore, a distinct increase of the drain current (I_D) allows the TFT to be turned on at any value of gate voltage with an on/off ratio of 1.41. Supplementary Fig. 3 and Table 1 summarize all the detailed parameter variations suggesting that the presence of DNA enhances the conductivity of IZO TFTs. As a result, the IZO TFT exhibits a substantial sensitivity with a quantitative response to the concentration of DNA which is hardly fulfilled by a biosensor based on electrostatic force.

We interpret this phenomenon as a result of the DNA oxidation associated with the reactive oxygen species on the IZO surface that supplies excessive carriers to the device. Eveleigh et al. have shown that the oxidation mechanism of DNA is related to the reactive oxygen species such as hydroxyl, peroxide, superoxide, and peroxynitrite adsorbed on the surface of transition metal oxide (Aust and Eveleigh, 1999). One of the most abundant and easily measured oxidation processes originates from guanine bases, in which the electron transfer process occurs in consecutive steps with the formation of oxidation products and dimmers on the surface of the metal oxide (Armistead and Thorp, 2001; Aust and Eveleigh, 1999; Hallaj et al., 2009). In this respect, the oxidation of guanine on the metal oxide would be useful for the design of nucleic acid biosensors.

To study the oxidant potential of our low-temperature processed IZO thin-film, Fourier transform infrared (FT-IR) spectroscopy was carried out with varied process temperatures of 100 °C (5 min), 280 °C (4 h), and 450 °C (3 h) as depicted in Fig. 3(a). Each annealing condition indicates the pre-annealed state and the post-annealed state of the low-temperature process, and the high-temperature process, respectively. In the spectrum of 100 °C (black), the peaks at 1709 cm^{-1} and 1591 cm^{-1} were assigned as the stretching vibration of C═O. Also, the peaks at 1328 cm^{-1}, 1097 cm^{-1}, and 1019 cm^{-1} represented organic functional groups in 2ME, most of which disappeared in 450 °C annealed sample (blue). On the other hand, in the spectrum of 280 °C (red), some residual still remained at 1276 cm^{-1}, 1103 cm^{-1}, and 830 cm^{-1} owing to NO_3^- deformation, which imply that there are plenty of reactive oxygen species on the surface of IZO to oxidize the DNA (Mayo et al., 2004; Nakamoto, 1997; Pashchanka et al., 2010).

The X-ray diffraction (XRD) patterns in Fig. 3(b) underpin that the DNA had no effect on the phase of IZO, confining the oxidation process to interact within the adsorbed chemical species on the surface. In conclusion, the high-temperature process at 450 °C constructs a sufficient quality of metal oxide with a reasonably small amount of the residual to ensure the performance of TFTs. However, in terms of their sensing ability, the reduction of these residuals lead to low reactivity with DNA, thereby diminishing its sensitivity (Jung et al., 2013; Kim et al., 2012). Additionally, IZO is expected to create a reactive oxygen species more frequently compared to IGZO in which Ga ions form strong chemical bonds with oxygen due to its high oxygen affinity (Kim et al., 2010).

Fig. 4 depicts a sensing mechanism on the basis of DNA oxidation, followed by the supply of excess electrons. During the oxidation process, guanine converts to intermediates such as 8-oxo7,8-dihydroguanine which leads to a further oxidation process (Hallaj et al., 2009). Accordingly, enough amount of electron is provided to increase the conductivity of the IZO thin-film, and the

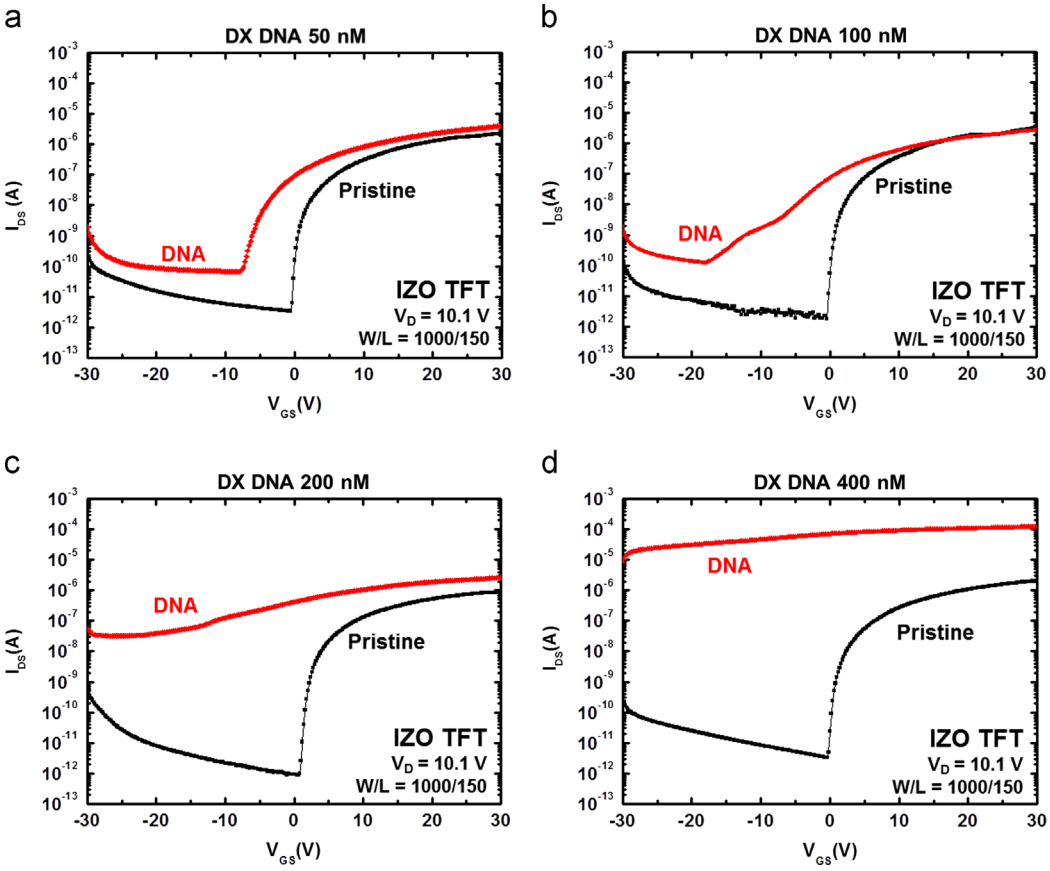

Fig. 2. Transfer characteristics of the low-temperature solution-processed IZO TFT based biosensors before and after DX DNA immobilization with varying concentrations of (a) 50 nM, (b) 100 nM, (c) 200 nM, and (d) 400 nM.

Table 1
Comparison of the electrical characteristics of low-temperature solution-processed IZO TFT based biosensors before and after immobilization of DX DNA with different concentrations.

Parameters	DNA 50 nM		DNA 100 nM		DNA 200 nM		DNA 400 nM	
	Original	DNA	Original	DNA	Original	DNA	Original	DNA
μ_{FET} (cm^2/Vs)	0.05	0.04	0.08	0.04	0.02	0.02	0.04	6.25
I_{on} (μA)	2.32	4.05	3.25	2.78	0.867	2.66	2.06	122.13
V_{on} (V)	−0.8	−8.2	−0.4	−18	0.6	−26.6	−0.4	−30
V_{th} (V)	1.71	−4.63	3.43	−3.51	1.84	−15.55	1.08	−34.47
On/off ratio	6.94×10^5	6.04×10^4	1.87×10^6	2.27×10^4	1.02×10^6	8.33×10	6.32×10^5	1.41

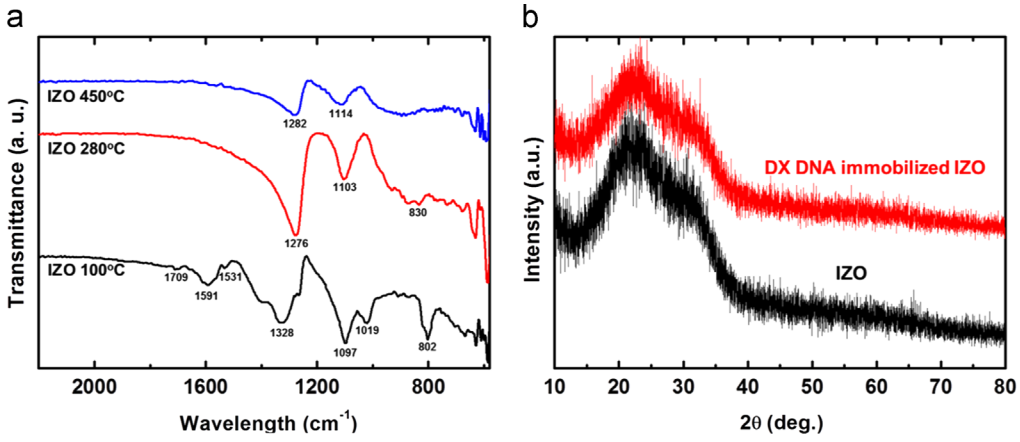

Fig. 3. (a) FT-IR of solution-processed IZO thin-film with annealing temperature of 100 °C, 280 °C, and 450 °C. (b) XRD pattern of solution-processed IZO thin-film before and after DX DNA immobilization.

aforementioned quantitative response of our biosensor corroborates this interpretation. The amount of supplied carriers followed the DNA concentration, leading to a subsidiary negative shift of V_{on} and increase of I_D, and even conductor-like behavior in the 400 nM case. This donor effect is tremendous enough that the electrostatic force from the phosphate groups can be ignored (Jung et al., 2013; Kim et al., 2012). The DNA oxidation based mechanism can be proved using DNA with controlled base such as adenine, thymine, cytosine and guanine oligomers. It is predictable that the variation of I_D after DNA immobilization follows the base sequence. We have executed the research about the selectivity of our biosensor with different types of oligomers and are planning to present the results in further study.

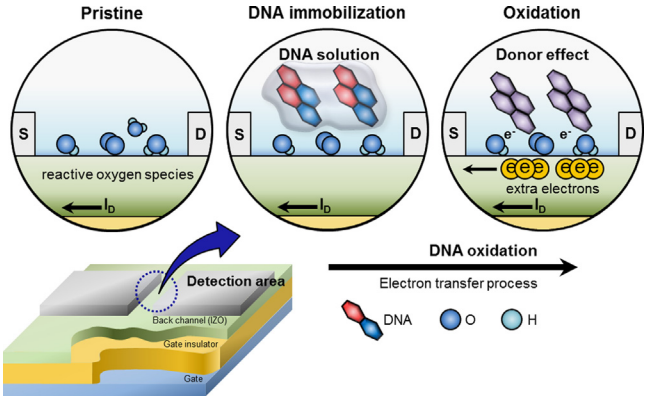

Fig. 4. Schematic diagram of the DNA oxidation on the solution-processed IZO TFT based biosensor.

Due to the low-temperature process of our IZO TFTs, a preferable route for applying flexible polyimide substrate was offered. Fig. 5(a) shows cross-sectional high-resolution transmission electron microscopy (HR-TEM) images of a flexible IZO TFT based biosensor and Fig. 5(b) and (c) depicts the compositional mapping of In and Zn constituents in which a uniform distribution was observed. Both of these figures substantiate that the homogeneous IZO thin-film was successfully performed at 280 °C without any thermal damage to the polyimide layer. Fig. 6 represents the sensing behaviors and optical images of our flexible biosensors which show completely identical tendencies with those of the Si substrate based biosensor. A negative shift of the transfer curve accompanying a diminishment in the on/off ratio and an enhancement of I_D became more exaggerated with increasing DNA concentrations from 25 nM to 100 nM. The flexible biosensor tends to be more sensitive to DNA which is believed to be induced by the different TFT structures; gate and gate insulator.

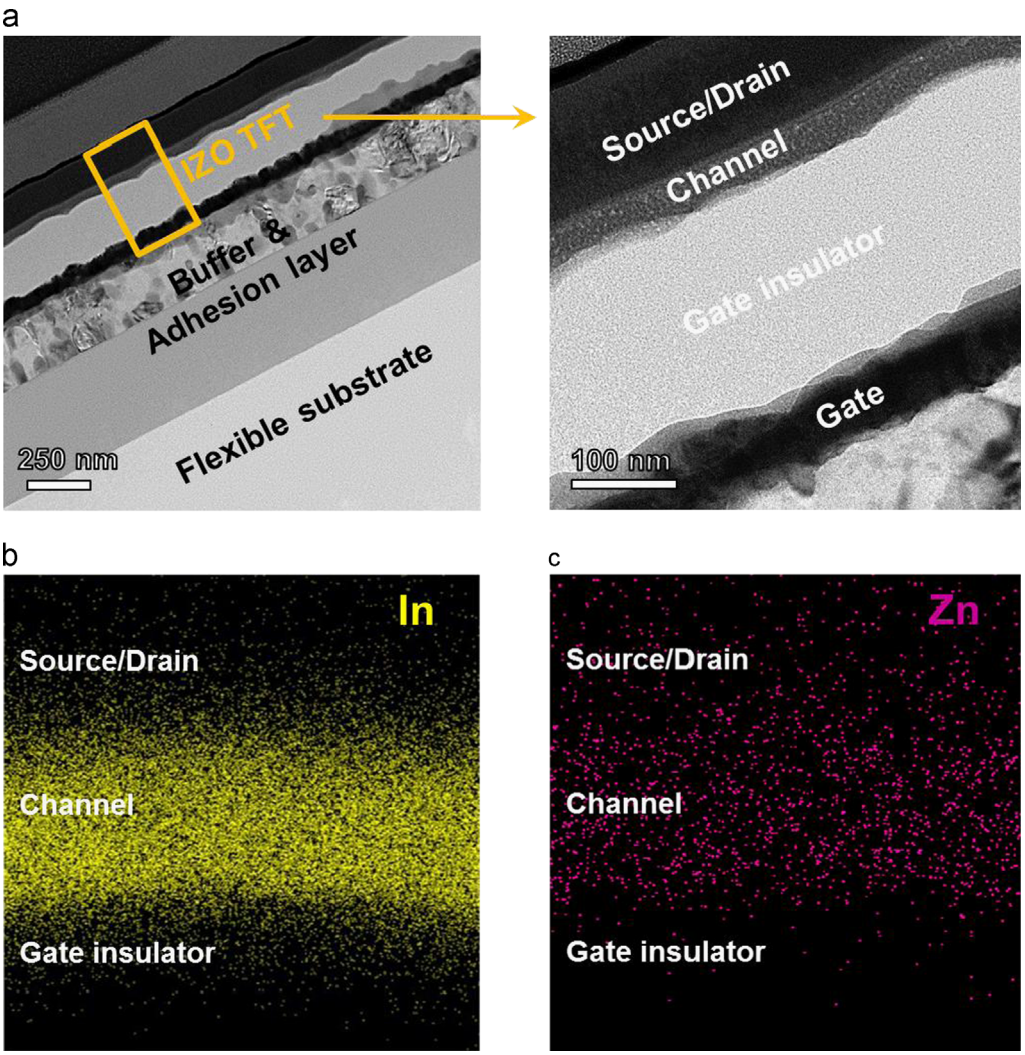

Fig. 5. (a) Cross-sectional HR-TEM images and compositional mapping of (b) In, and (c) Zn of flexible IZO TFT based biosensors.

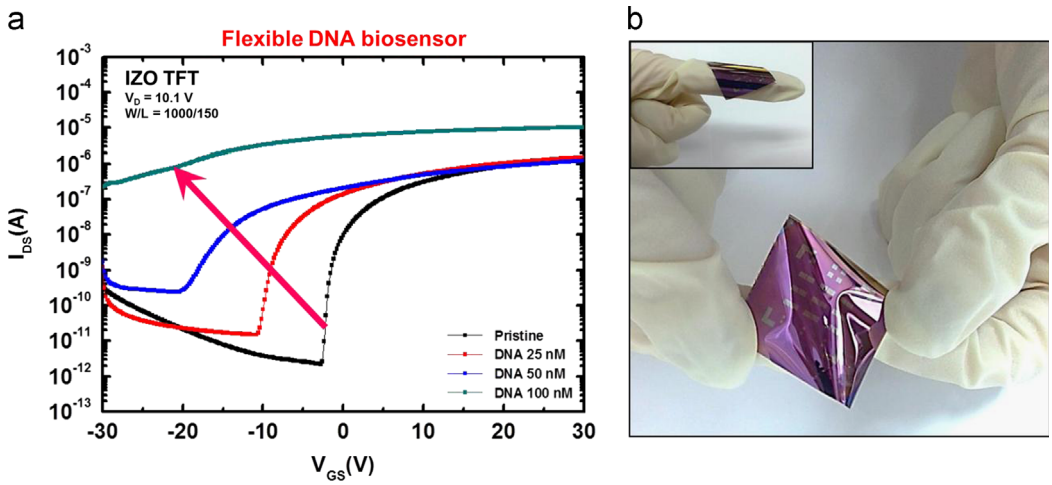

Fig. 6. (a) Transfer characteristics of the flexible low-temperature solution-processed IZO TFT based biosensors before and after DX DNA immobilization with varying concentrations of 25 nM, 50 nM, and 100 nM. (b) Optical images of flexible IZO TFT based biosensors.

Consequently, this low-temperature of 280 °C guarantees both magnificent adaptation to the polyimide substrate and its sensing mechanism based on the DNA oxidation at the surface of the IZO, raising the conductivity of the TFTs. As the concentration of the DNA solution increased, the variance of V_{on}, I_D, and the on/off ratio via the supplied electrons became more intense. This series of procedures that we have established is the origin of an outstanding sensitivity and a reasonable quantitative sensing response. The various DNA concentrations which cannot be distinguished by optical measurements such as XRD or transmittance (data not shown) were distinctly differentiated. This high sensitivity of IZO TFTs is additionally promoted by its amplifying characteristic of transistors to detect extremely small amount of DX DNA nanostructure without any change in its bulk state.

Compared with our previously reported IGZO based biosensor, there are notable superior features. At first, IZO requires relatively low-temperature annealing during the process compared with IGZO which needs high-temperature annealing. It makes it possible to realize the biosensor on the flexible polyimide substrate. Also due to reactive oxygen species on the IZO surface and absence of Ga in its lattice, the sensing behavior is derived from the DNA oxidation instead of electrostatic force, and this allows quantitative analysis between various concentrations of DNA and also contains possibility of selective sensing in terms of guanine. As a consequence, this would extend the portability, adaptability and even the mechanical strength of a biosensor aiming at the next generation biosensor market. Furthermore, on the basis of its selective behavior to the DNA sequence, the IZO based biosensor represents promising candidate for the diverse biological tools such as diagnosis the genetic mutation related disease, detection of bacteria, and even forensic medicine in the near future (Du et al., 2009; Hammock et al., 2013; Luo et al., 2013).

4. Conclusion

In summary, we have demonstrated flexible DNA biosensors based on the low-temperature solution-processed IZO TFTs with a superior signal to-noise ratio and also a clear quantitative analysis. The immobilized DX DNA nanostructures were oxidized on the IZO channel surface causing the electron transfer process. The oxidation motivated a significant increase in the conductivity in the transfer curve embodying a negative shift of V_{on}, a decrease of the on/off ratio, and an increase of I_D. As a result, we strived to implement our IZO TFTs as a flexible biosensor which concluded with a satisfactory result; still the vast fields to be researched are remaining.

Acknowledgment

This work was supported by the National Research Foundation of Korea (NRF) grant funded by the Korean Ministry of Education, Science and Technology (MEST) [no. 2011-0028819].

Appendix A. Supplementary material

Supplementary data associated with this article can be found in the online version at http://dx.doi.org/10.1016/j.bios.2013.11.076.

References

Armistead, P.M., Thorp, H.H., 2001. Anal. Chem. 73 (3), 558–564.
Aust, A.E., Eveleigh, J.F., 1999. Exp. Biol. Med. 222, 246–252.
Boon, E.M., Salas, J.E., Barton, J.K., 2002. Nat. Biotechnol. 20, 282–286.
DeRisi, J.L., Iyer, V.R., Brown, P.O., 1997. Science 278, 680–686.
Du, P., Li, H., Mei, Z., Liu, S., 2009. Bioelectrochemistry 75, 37–43.
Hallaj, R., Salimi, A., Akhtari, K., Soltanian, S., Mamkhezri, H., 2009. Sens. Actuator B: Chem. 135, 632–641.
Hammarberg, E., Prodi-Schwab, A., Feldmann, C., 2009. J. Coll. Interface Sci. 334, 29–36.
Hammock, M.L., Knopfmacher, O., Benjamin, D.N., Tok, J.B.-H., Bao, Z., 2013. ACS Nano 7 (5), 3970–3980.
Honeychurch, K.C., O'Donovan, M.R., Hart, J.P., 2007. Biosens. Bioelectron. 22, 2057–2064.
Jung, J., Kim, S.J., Yoon, D.H., Kim, B., Park, S.H., Kim, H.J., 2013. ACS Appl. Mater. Interfaces 5, 98.
Kim, G.H., Jeong, W.H., Kim, H.J., 2010. Phys. Status Solidi A Appl. Mater. Sci. 207 (7), 1677–1679.
Kim, S.J., Kim, B., Jung, J., Yoon, D.H., Lee, J., Park, S.H., Kim, H.J., 2012. Appl. Phys. Lett. 100, 103702.
Kim, S.J., Jung, J., Yoon, D.H., Kim., H.J., 2013a. J. Phys. D: Appl. Phys. 46, 035102.
Kim, S.J., Jung, J., Lee, K.W., Yoon, D.H., Jung, T.S., Dugasani, S.R., Park, S.H., Kim, H.J., 2013b. ACS Appl. Mater. Interfaces 5, 10715–10720.
Kosmulski, M., 2001. J. Coll. Interface Sci. 238, 225–227.
Lee, K.W., Kim, K.M., Lee, J., Amin, R., Kim, B., Park, S.K., Lee, S.K., Park, S.H., Kim, H.J., 2011. Nanotechnology 22, 375202.
Luo, C., Tang, H., Cheng, W., Yan, Li, Zhang, D., Ju, H., Ding, S., 2013. Biosen. Bioelectron. 48, 132–137.
Mayo, D.W., Miller, F.A., Hannah, R.W., 2004. Course Notes on the Interpretation of Infrared and Raman Spectra, first ed. Wiley.
Nakamoto, K., 1997. Infrared and Raman Spectra of Inorganic and Coordination Compounds, fifth ed Wiley.
Newman, J.D., Turner, A.P.F., 2005. Biosens. Bioelectron. 20, 2435–2453.

Pashchanka, M., Hoffmann, R.C., Gurlo, A., Schneider, J.J., 2010. J. Mater. Chem. 20, 8311–8319.
Reyes, P.I., Ku, C.-J., Duan, Z., Lu, Y., Solanki, A., Lee, K.-B., 2011. Appl. Phys. Lett. 98, 173702.
Sharma, H., Mutharasan, R., 2013. Sens. Actuators B 183, 535–549.
Shin, J., Kim, J., Amin, R., Kim, S., Kwon, Y.H., Park, S.H., 2011. ACS Nano 5 (6), 5175–5179.
Singh, N.P., McCoy, M.T., Tice, R.R., Schneider, E.L., 1988. Exp. Cell Res. 175, 184–191.
Turner, A.P.F., 2013. Chem. Soc. Rev. 42 (8), 3184–3196.
Xuan, F., Luo, X., Hsing, I.-M., 2012. Biosens. Bioelectron. 35, 230–234.
Yan, F., Tang, H., 2010. Expert Rev. Mol. Diagn. 10 (5), 547–549.
Zhang, J., Song, S., Wang, L., Pan, D., Fan, C., 2007. Nat. Protoc. 2 (11), 2888–2895.
Zuo, X., Xia, F., Xiao, F., Plaxco, K.W., 2010. J. Am. Chem. Soc. 132, 1816–1818.